VACUUM FORMED GFRP PROFILES USED AS EXTERNAL REINFORCEMENT IN DAMAGED CONCRETE SCTRUCTURES – LOW COST APPROACH

A. Ortenzi[1]; M. A. Ferreira[2]; J. Carvalho[1]
1 – University of Sao Paulo - USP
2- Federal University of São Carlos - UFSCar
Av. Trabalhador São-carlense 400, São Carlos. 13566-590, Brazil
ortenzi@sc.usp.br, maferreira@ufscar.br, prjonas@sc.usp.br

SUMMARY

The knowledge of damaged beams is important to predict the behavior of the real structural members and how the structure can be affected by damages. In this work it was simulated and analyzed experimentally the behavior of reinforced concrete beams after they have been tested up to ultimate limit state (ULS) and then reinforced by vacuum formed GFRP composites. Initially the undamaged beams were simulated using finite element analysis and the results compared to the experimental ones. Next, the ULS load reached in the test is applied to the reinforced beams and simulated with the FEM package. The final results are compared and discussed.

Keywords: vacuum form GFRP, composite, FEM, precast concrete

INTRODUCTION

Many works around the world are conducted to predict the capabilities of retrofit reinforcements in columns and beams damaged by impact of trucks, seismic actions or by the degradation caused by salt used over the snow, especially in north hemisphere [1] and [3]. One of the main benefits of the GFRP reinforcements to prevent or repair structures is its rapid liberation for the traffic. This means hours against one or two days when using conventional grout or concrete. Many researchers have found several retrofit systems to prevent and repair structural precast concrete members. The goal of this work is to simulate and to compare the results of a specific profile used as external reinforcement. This profile is fixed by adhesion and post laminate anchorage using shear connectors to prevent the sliding of the reinforcement. Two precast beams with the geometry of the Figure 1 were reinforced. This beam, named as B1, was collapsed by tests that have been carried out up the Ultimate Limit State - ULS [4] respect with the domains 3 and 3 to 4, [6]. The other beam, named as B2, was numerically simulated by using the results obtained in four point flexural test with the B1. The flexural test was carried out initially to know the capabilities of these structural members at the ULS. The Table 1 gives the test results for the part B1. This work simulated different procedures to reinforce the beams in order to select the GFRP profile that could provide the largest bending strength and stiffness for the damage beams. After the selection of the best profile a vacuum formed mold was built. Next, the beams were prepared to receive the reinforcement. Finally, it was conduced bending tests in the beams in order to verify their structural behavior.

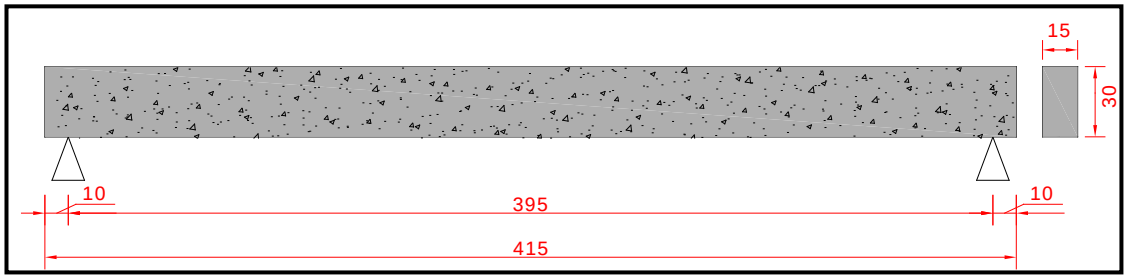

Figure 1 – Geometry of tested precast beams, [4].

Initial Stage

The beams were named B1 and B2, the first was used as parameter of control, without GFRP reinforcement and the second has received the reinforcement with the geometry shown in Figure 2. The test carried out in the B1 is known by Stuttgart Test [4], and it is shown in Figure 2. The actuator force is applied at the mid spam of the beam and it is propagated by a transfer beam between two points that receive one half of the applied force each one. This method is used to provide only the flexural reaction at mid spam and to isolate other secondary effects that occur if the load is applied concentrated on the mid spam.

The Table 1 shows the properties of the materials used to construct the beam used to test.

Table 1 – Mechanical properties of the materials used to construct the beam B1.

Material	E (GPa)	Poisson	Ultimate Compressive Strength (MPa)	Ultimate Tensile Strength (MPa)
Steel	210	0,2	460	460
Concrete	35,4*	0,22	40	3,5

* The Young modulus of the concrete for design purposes is given in literature and Brazilian standard, [5], [6].

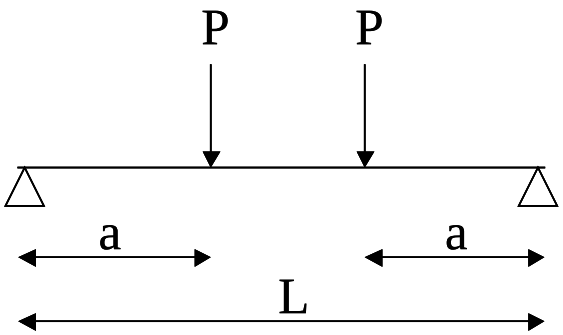

Figure 2 – Setup of the Stuttgart Test used to test the beam B1, [4].

The results of the damaged condition on the beam B1 is shown in Table 2, Figures 3 and 4.

Table 2 – Force in actuator versus deflection at the rupture of the B1.

Force in actuator (kN/2)	Deflection (mm)
27.0	23.6

The damaged beam B1 is shown in Figure 3 at the stage 2 (low ratio of reinforcement) and the Figure 4 shows the plotting of the moment versus deflection at rupture.

Figure 3 – B1 with cracks propagated after the test – Numbers represents the actuator force at the crack propagation in kN, [4].

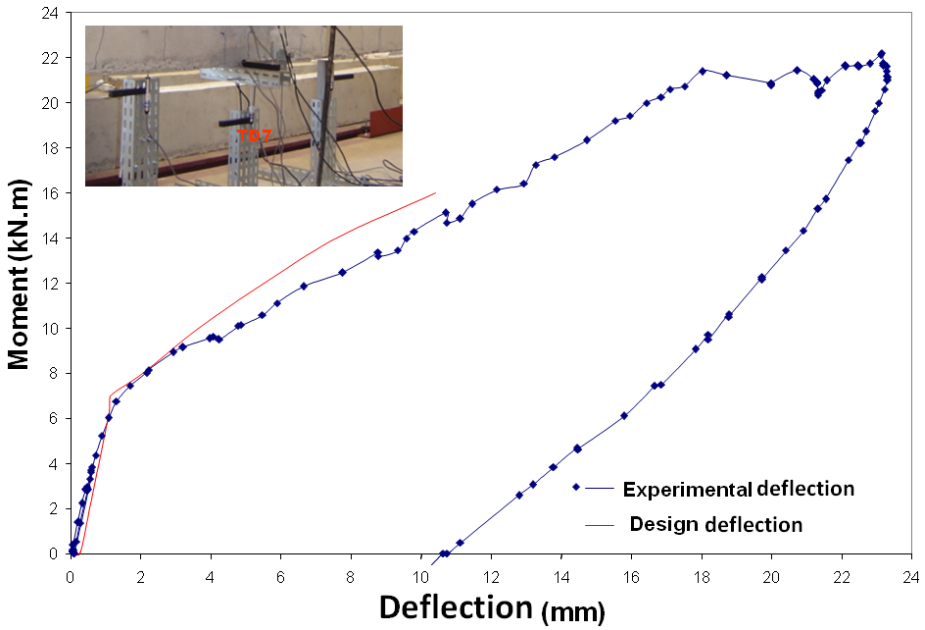

Figure 4 – Moment versus deflection plotted at the mid spam of the B1, [4].

The next step was the simulation of condition of damage occurred in the B1 beam using commercial FEM software. It was used the NASTRAN/PATRAN solver and modeler, respectively. The real loads and deformations were shown in the Table 3. These results are the basis to start the new tests with retrofit reinforcement with GFRP [1]. After the

application of the external reinforcement the beams were loaded up to the maximum value achieved at normal conditions. The goal of the tests was to improve the capability of the beams to preserve the strength and stiffness when reload after their failure at ULS.

Simulation

The simulation was conducted at the Department of Mechanical Engineering in the São Paulo University - USP, using the FEM application MSC NASTRAN / PATRAN [2]. The simulation has been used to verify more precisely the effects of the GFRP capability according to its geometry and to verify the convergence of the numerical results with the tested ones.

The first step was to simulate the same beam without external reinforcement to know possible divergences between the test and the numerical analysis. As result, the simulation presented a small difference regarding the test conducted. The difference was about 3.9% greater than the actual deflection presented in B1 test.

The input data are based in literature. The fiber fraction was defined as 65% in volume and it was used based in mixtures rule and also on plies failure criteria, [8], [9] and [10]. Therefore, the external design reinforcement is a GFRP profile produced by the vacuum form system, shown in Figure 5. The fiber used in the structural design was the ADVANTEX® [13] roving with 600 g/ sqm. The Table 3 shows the properties of the laminate.

Table 3 – General properties of the laminated GFRP profile.

Fiber (g/sqm)	Orientation	Polymer	Thickness	V_f (%)	Plies
600	0° / 90°	Vynilester	9 mm	65	11

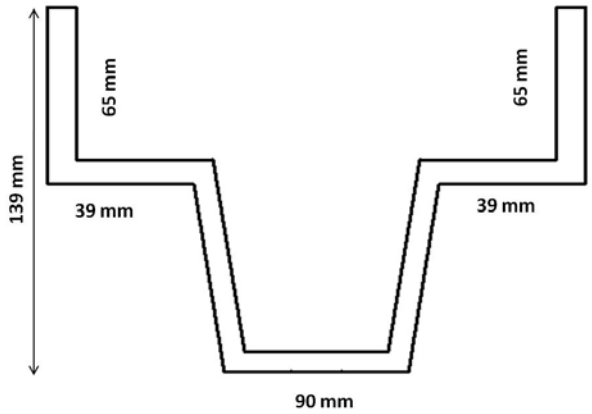

Figure 5 – GFRP Profile used in simulation as external reinforcement of the B2.

The estimated mechanical properties of the composite based in literature, [8], [9], [12] and [13], are shown in Table 4.

Despite the anisotropy of composites, in this work the profile was considered as orthotropic material in the plane of the laminate.

Table 4 – Mechanical properties of the GFRP profile.

E_x (GPa)	E_y (GPa)	E_z (GPa)	Poisson xy	Poisson yz	Poisson xz	G_{xy}	G_{yz}	G_{zx}
58	18,6	18,6	0,36	0,26	0,26	4,2	5,6	5,6

The Figures 6, 7, 8 and 9 show the mesh, the applied load, the total displacement and the maximum strain, respectively, of the B1 beam when simulated with the NASTRAN®.

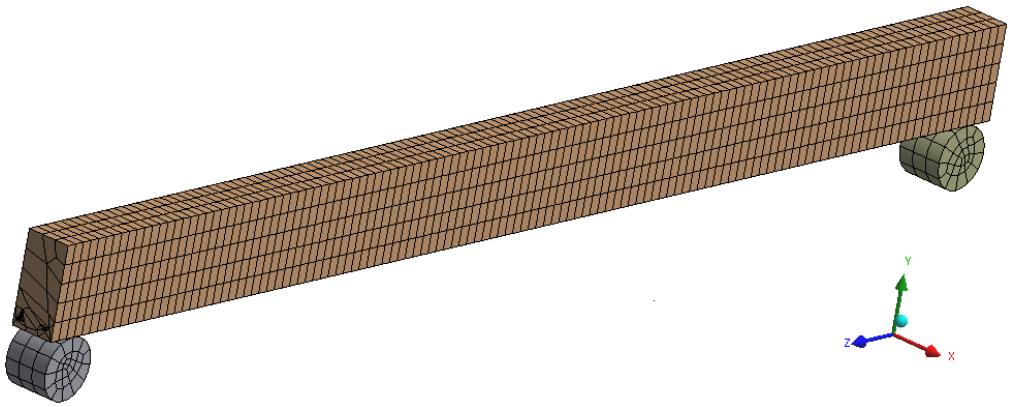

Figure 6 – B1 beam reinforced only with steel rebars – meshed with hexa geometry.

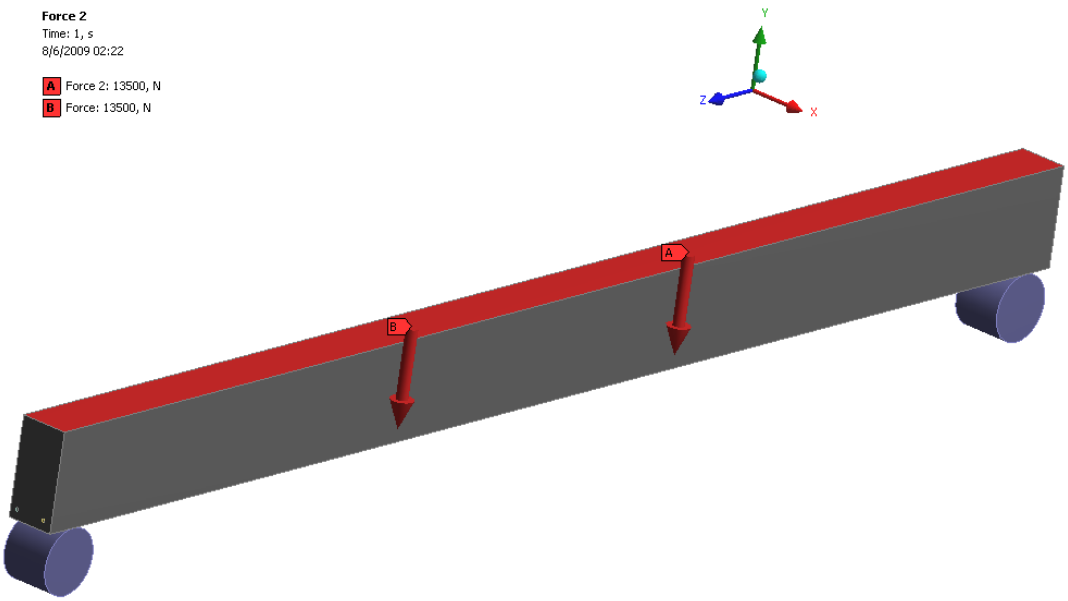

Figure 7 – Applied load on simulated model without external reinforcement.

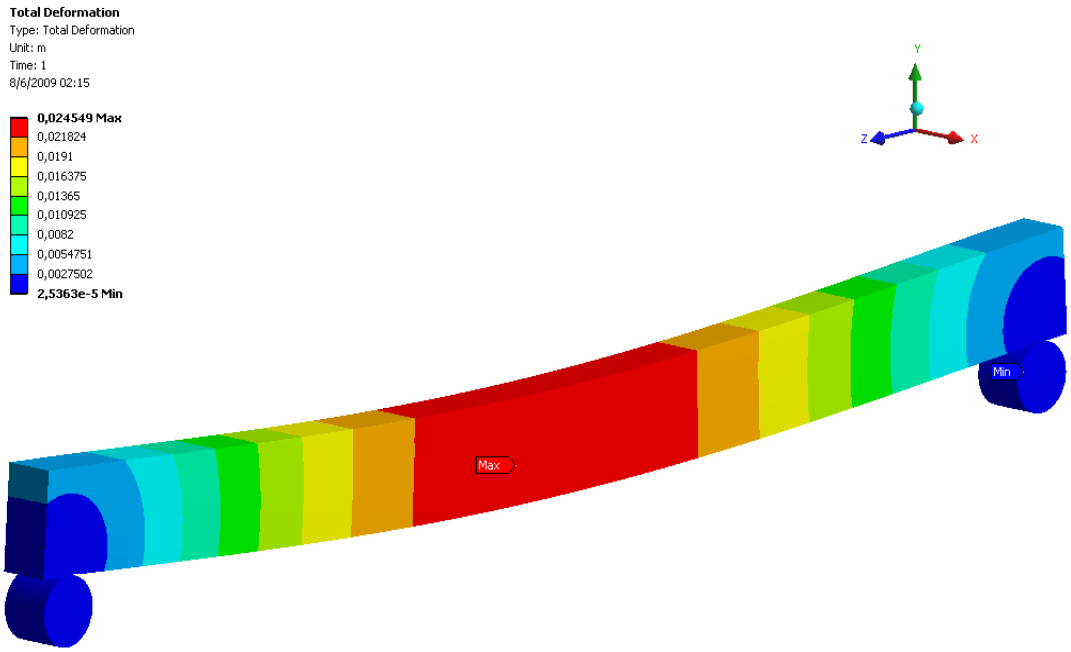

Figure 8 – Total deflection of B1 based on data of model test.

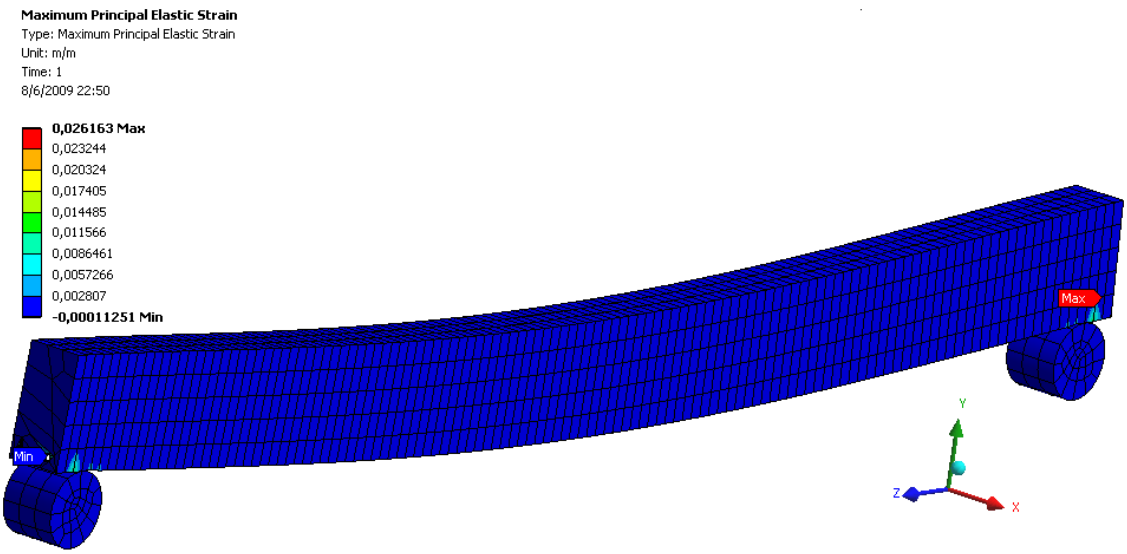

Figure 9 – Maximum principal elastic strain in B1 simulation.

Next, using the GFRP profile shown in Figure 5 above, a new simulation was done. In this second analysis it was included the GFRP profile as external reinforcement to compare mainly the deflection and strain in the same structural member, considering the B1 beam undamaged (in the first case) and the B2 beam damaged and retrofitted by the external reinforcement (in the second case) . Due to the complexity of the models required, the shear reinforcement was not included. The same was done with the GFRP profile that was considered as bonded in contact surface between the profile and the beam.

The Figures 10, 11, 12 and 13 show the mesh of the B2, the applied load, the deflection and the maximum strain for the same boundary condition but with the GFRP profile as external reinforcement.

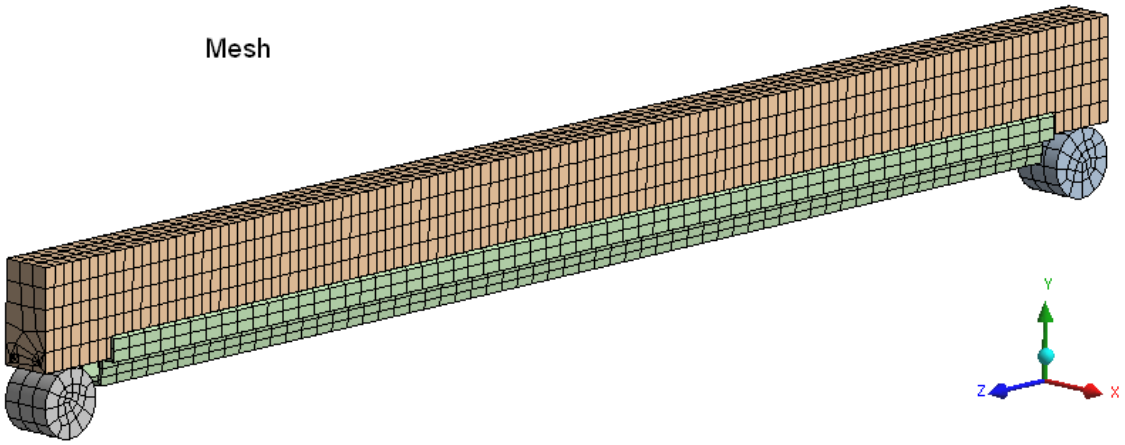

Figure 10 – Mesh of the B2 reinforced externally by a GFRP Profile.

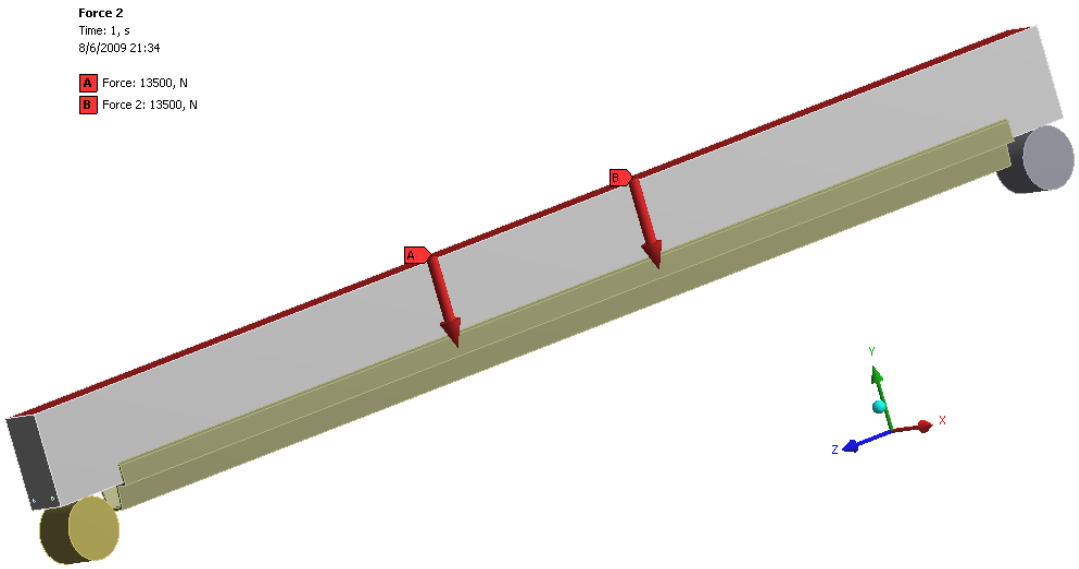

Figure 11 – Applied load on B2 to simulate the capability of external reinforcements..

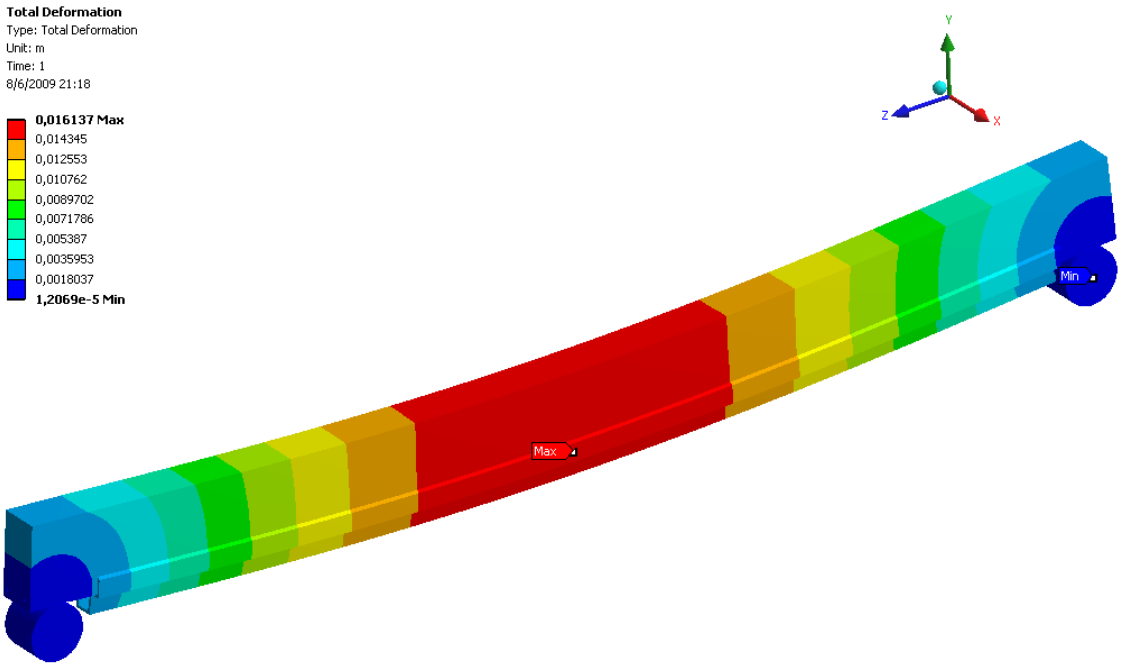

Figure 12 – Total deflection in B2 – The applied load was the same in all case studied.

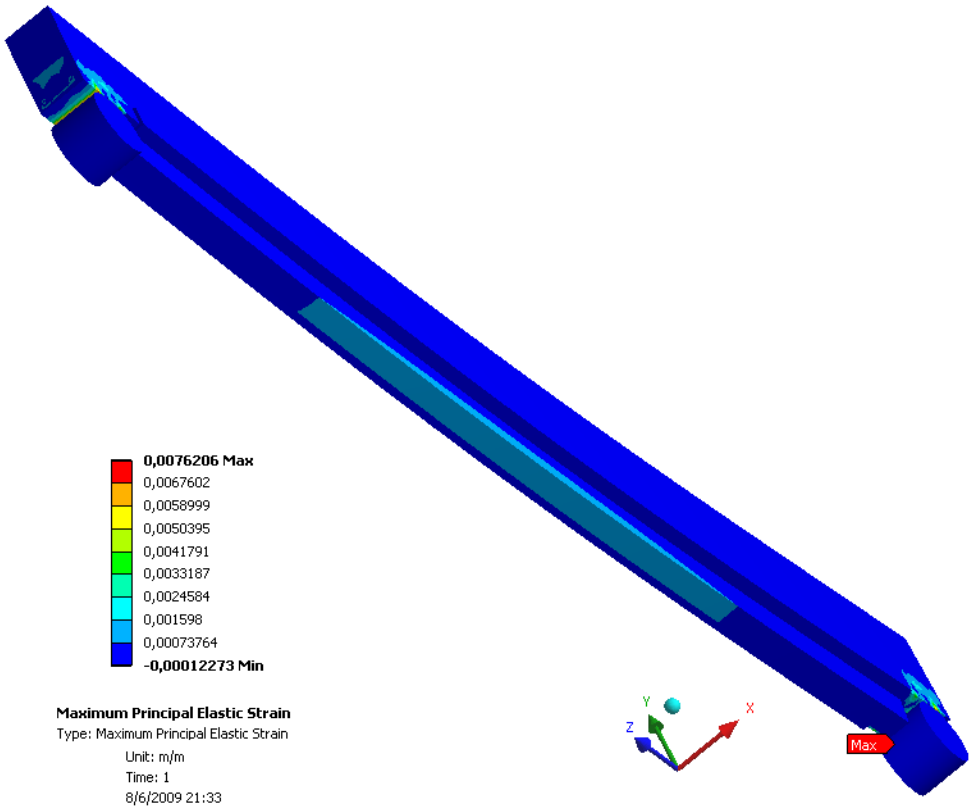

Figure 13 – Maximum strain in B2.

Comparison Between Experimental and Simulated Results

Here are presented the two simulated situations. In first case the simulation

To experimental and numerical results are compared as shown in the Table 5.

Table 5 – Compared results from B1 and B2.

Member	Force (kN)	Deflection (mm)	Strain (mm/mm)
B1*	27	23,6	2,54
B1	27	24,5	16,14
B2	27	16,13	7,62

* Real member tested as described before and used as control parameter..

As shown in Table 5, the total deflection of the B1 beam was 152% greater than the deflection of the B2, with external reinforcement. In the same way, the strain in B1 was 211% greater than the strain of the B2 for identical load and boundary conditions.

The deflection of the B1* was greater than both of the other simulations but the strain was much lower than the simulated beams. This fact may be due to the interface between the steel rebars and the concrete of the simulated beams and their contact surface.

As expected, the bottom face of the GFRP profile was much more deformed than the other faces. This fact is due to the traction in the lower fibers. But at the same time the stresses acting in the bottom face of the beam shows that the support region will be collapsed and presents the maximum strain in both cases.

Results and Discussions

This work compared the results of tests carried out in a beam at the ULS with respect to another with the same geometry reinforced by a GFRP profile. The reinforced beam had a significant improvement of its structural capability. The next step is to apply the GFRP profile in a damaged beam to test the ability of the structural member to recover their serviceable strength.

It wasn’t considered the friction coefficient in traction of the rebars. This study must be done in further researches to improve the mechanisms to restrict the displacement of the reinforcement steel rebar and their surface of contact with the beam’s concrete.

ACKNOWLEDGEMENTS

The authors acknowledge the REICHHOLD® by the donation of the polymer, the OCV® by the donation of the ADVANTEX® Glass Fiber and to the MSC by the use of the NASTRAN/PATRAN Academic version.

References

1. A. J. Boyd. **Sprayed Fibre Reinforced Plastics for Repairs.** Ph.D. Thesis. Department of Civil Engineering. The University of British Columbia, Vancouver, Canada, 2000.
2. MSC. NASTRAN / PATRAN – Finite Elemente Analysis and Modeling Software. McNeal Company. Santa Ana, USA: MSC, 2009.
3. K. Rehm. **Full Scale Testing of FRP Repaired Prestressed Beams.** AASHTO - American Association of State Highway and Transportation Officials. Washington, USA, AASHTO, 2005.
4. M. A. Ferreira; C. A. T. Justo. **Metodologia para Medição da Rotação e Curvatura na Zona de Distúrbio na Extremidade de Vigas Pré-moldadas de Concreto.** Iniciação Científica. São Carlos: UFSCar, 2006.
5. R. C. Carvalho; J. R. de Figueiredo F°. **Cálculo e Detalhamento de Estruturas Usuais de Concreto Armado.** 3rd. Ed. São Carlos: EDUFSCAR, 2007.
6. ABNT. Brazilian Standard Association. **NBR – 6118- 2003**. Rio de Janeiro: ABNT, 2003.
7. J. C. Sussekind. **Curso de concreto armado**. V. I e II. São Paulo: Globo, 1989.
8. M. Piggott. **Load Bearing Fibre Composites, 2nd Ed**. Ontario: KLUWER ACADEMIC PUBLISHERS, 2002.
9. S. W. Tsai. **Theory of Composites Design and MICMAC-Lite V2**. STANFORD: S. W. Tsai, 2004.
10. A. B. Shultz; S. W. Tsai. **Measurements of Complex Dynamic Moduli for Laminated Fiber-Reinforced Composites**. Journal of Composite Materials. 1969; 3; 434**.** Ohio: SAGE Publications, 1969.
11. A. Ortenzi. **The Glass Fiber in Polymeric and Cimenticious Matrix and their Use as Structural Reinforcement in Civil Construction – The State of Art**. Mastering Dissertation. São Carlos, Brazil: UFSCar, 2007.
12. M. W. Hyer. **Stress Analysis of Fiber-Reinforced Composite Materials.** Virginia: WCB – McGraw-Hill, 1998.
13. OCV. Owens Corning – VETROTEX. **Mechanical Properties of the ADVANTEX Roving.** Rio Claro: OCV, 2009.
14. O. O. Ochoa; J. N. Reddy. **Finite Element Analysis of Composite Laminates.** Texas: KLUWER Academic Publishers, 1992.